Electronic Supplementary Information for *Dalton Trans.*

A series of Zn–4f heterometallic coordination polymers and zinc complex containing flexible mixed donor dicarboxylate ligand

Xun Feng,[a] Yu-Quan Feng,[b] Lang Liu,[c] Li -Ya Wang,[*a, b]
Hong-Liang Song,[a] Seik-Weng Ng [d]

1 Experimental detail

1.1 Syntheses of organic ligand

Ligand *H_2PBDA* was prepared by modification of the literature method previously reported by H. Vicente [1] from the reaction of 3-nitrophthalonitrile with pyridine substituent in situated, in the presence of excess zinc acetate, in the 63 % yield, followed by hydrolysis, purification and further neutralization.

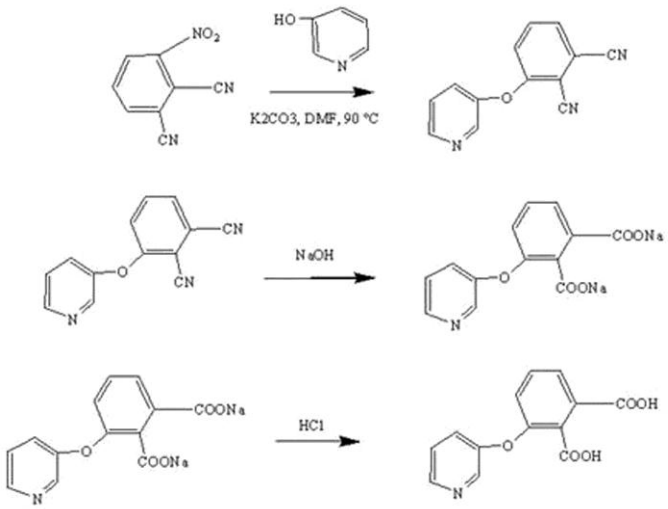

Scheme S1. Synthetic route of *H_2PBDA* ligand

1.2 Heat treatment and dehydration on sample 6

The freshly prepared sample of **6** was soaked in methanol for 3 days, and the extraction was decanted subsequently, the sample was collected by decanting and treated with dichloromethane similarly to to remove the water molecules, and then pumped under a dynamic vacuum at 140 ^{o}C over night subsequently to activate the samples.

2 Additional figures

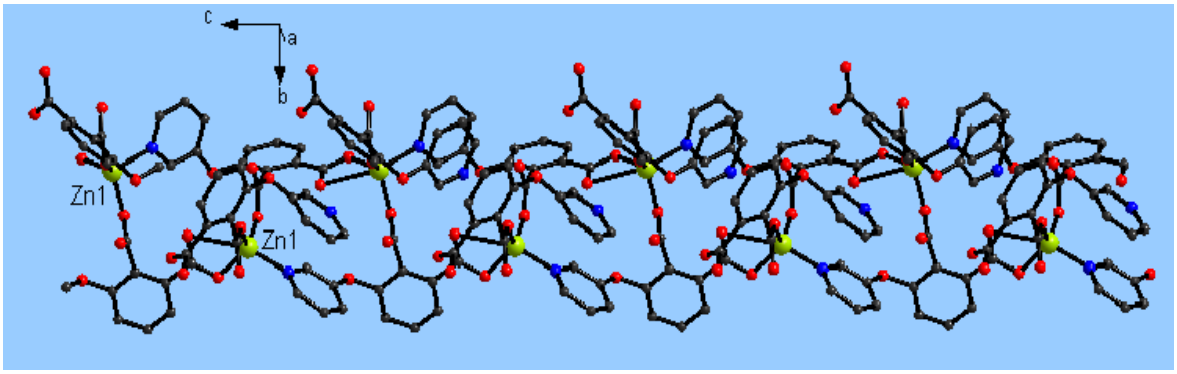

Figure S1. Illustration of 1D chain linked by *PBD*A anion ligands viewed approximately down *a b* plane in **1**

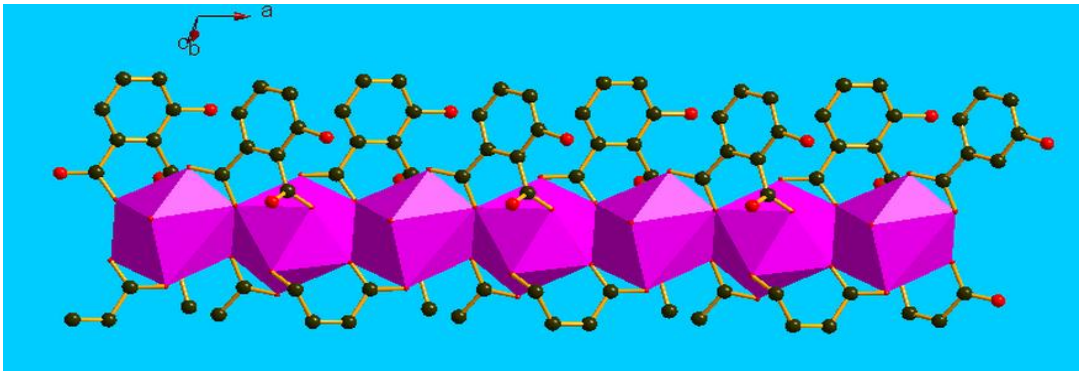

Figure S2. Illustration of phthalate propagating the Pr_2 dimeric units into 1D chain along a c plane in **2**

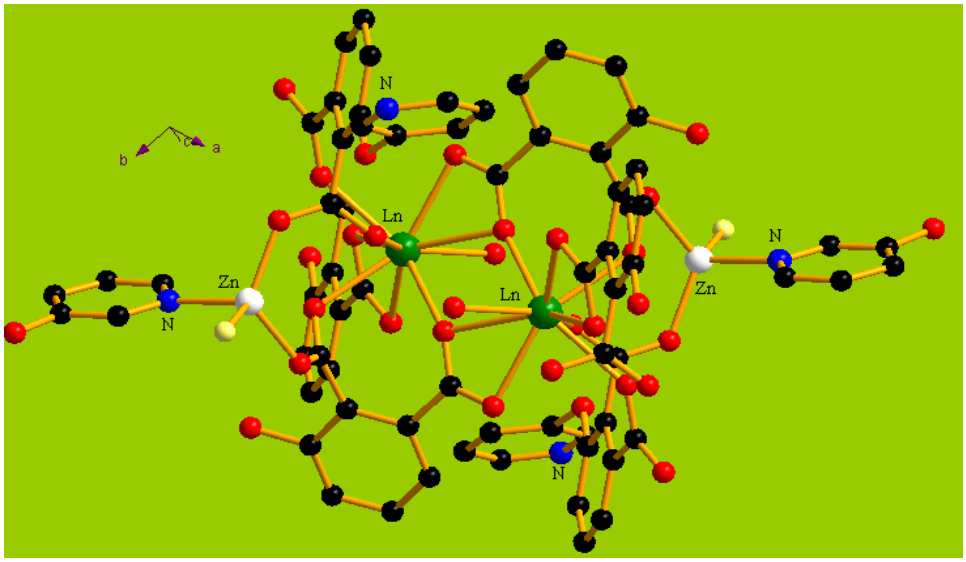

Figure S3. Projective view of an individual Ln_2Zn_2cluster in **2-7** viewed approximately down a *b* plane

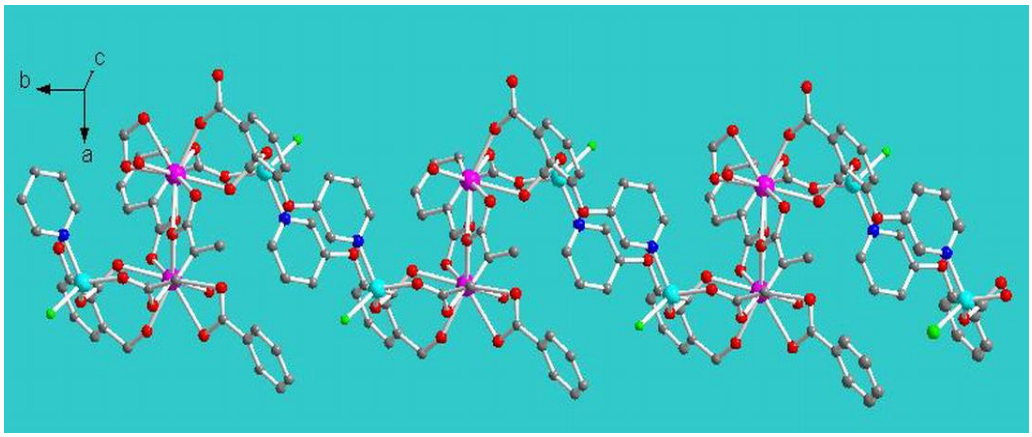

(a)

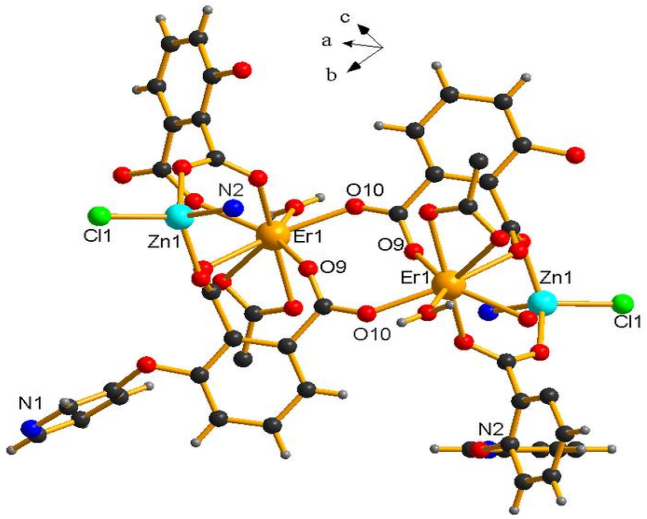

(b)

Figure S4 (a) Illustration of phthalate propagating the Pr_2Zn_2 cluster units into 1D zigzag chain in **2-7**. (b) Illustration of an individual Er_2Zn_2cluster in **8** viewed approximately down the *b* c plane with partial atomic number scheme

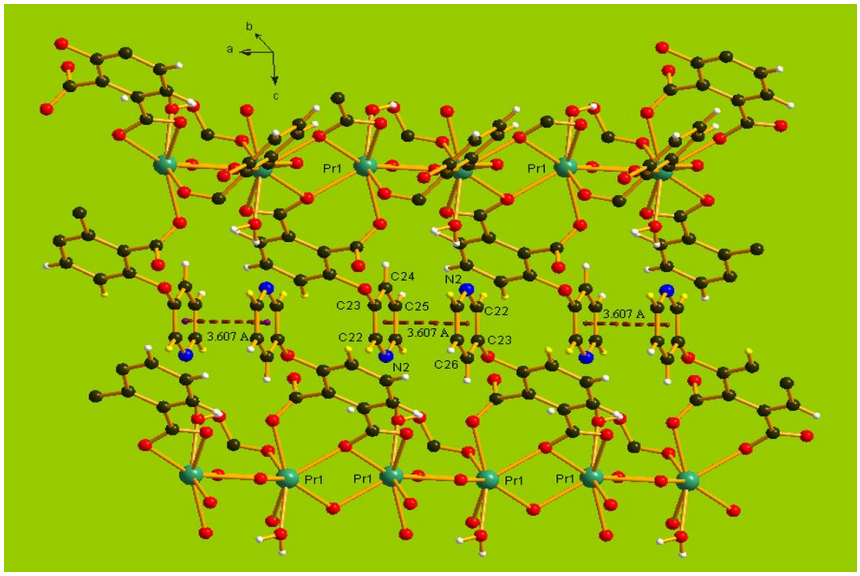

Figure S5. Packing diagram of complex **2** *via* the inter-chain π-π stacking interactions

From the Figure S4 (b), we can see in the symmetry unit of **8**, the central Er(III) ion is eight-coordinated rather than nine-coordinated, exhibiting distorted square-antprism geometry. Among the donor set, two oxygen atoms are from the carboxylic groups of PBDA ligand, adopting the mono dentate bridging coordination mode. Adjacent carboxylic groups were coordinated to Er (1) and produced a distorted eight numbered ring, acting as connecter, linking neighboring two Er (1) ions. Each of the two Zn(II) ions adopts an tetrahedron coordination environment with two oxygen atom from *PBDA*, one nitrogen of next *PBDA* and one chlorine anion.

PXRD Measurements andThermal gravimetric Analysis

The purity and homogeneity of the bulk products of **1-8** were determined by comparison of the simulated and experimental X-ray powder diffraction patterns of microcrystalline powders of **1-8**.

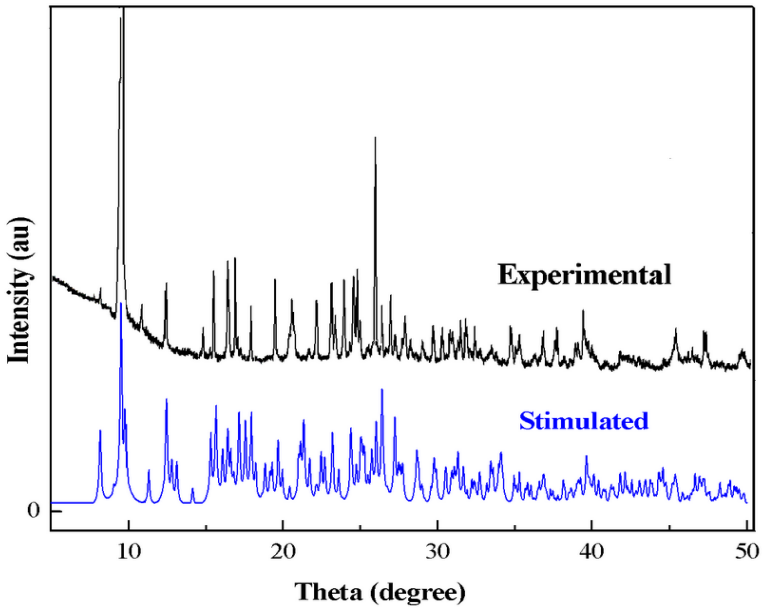

Figure S6. Simulated (lower trace) and experimental (upper trace) X-ray powder diffraction patterns of microcrystalline powders of complex **1**

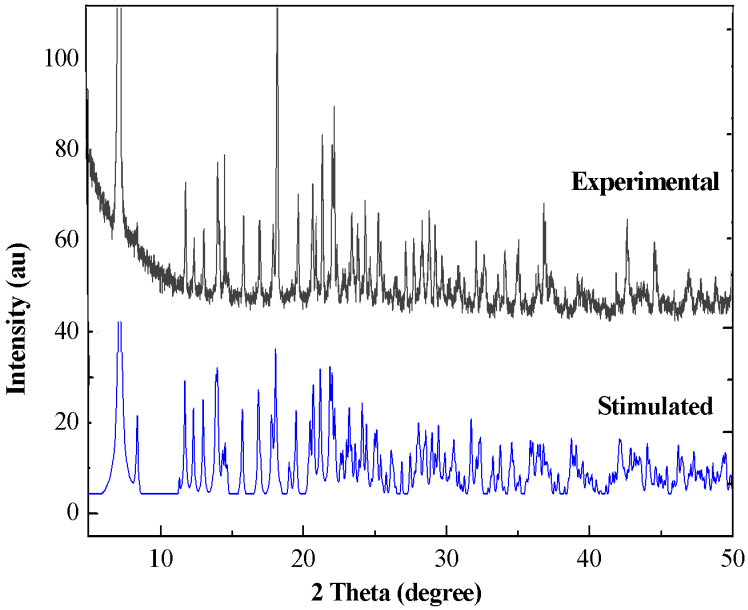

Figure S7. The X-ray powder diffraction diagrams of microcrystalline powders of **2**

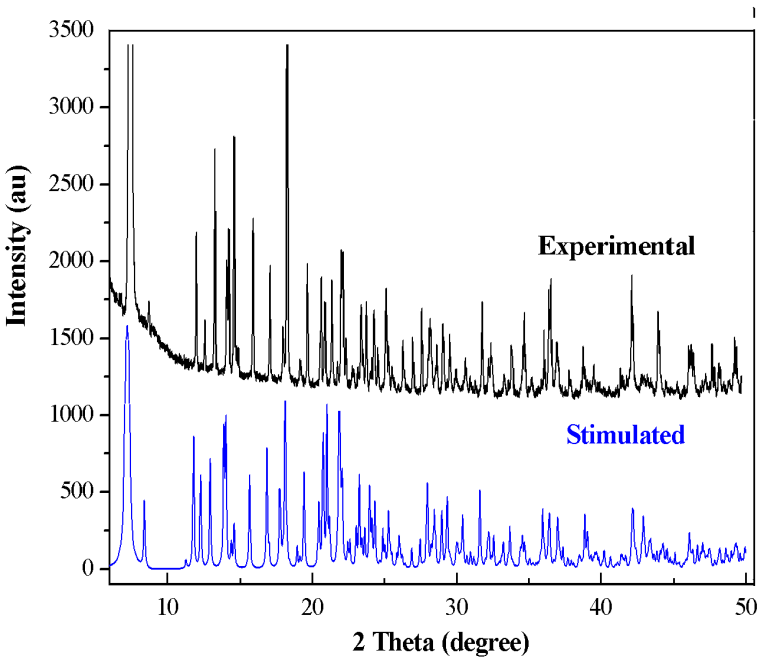

Figure S8. The X-ray powder diffraction diagrams of microcrystalline powders of **3**

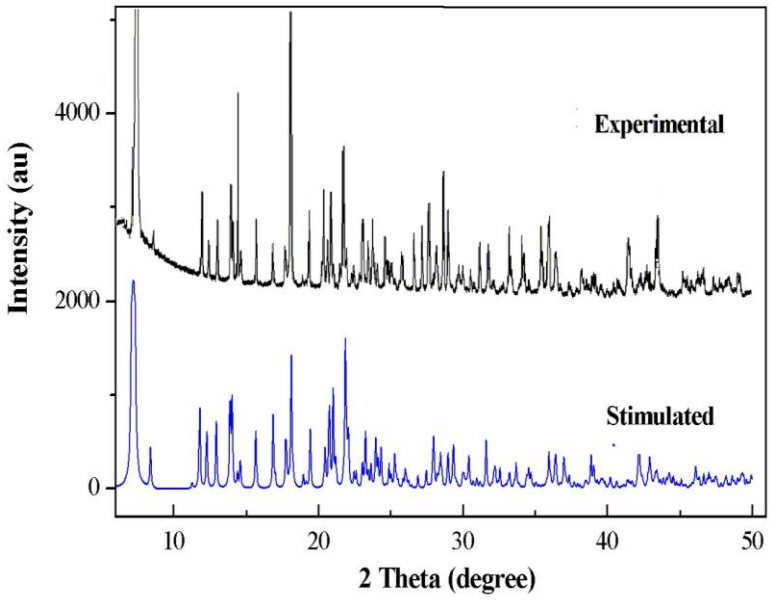

Figure S9. The X-ray powder diffraction diagrams of microcrystalline powders **4**

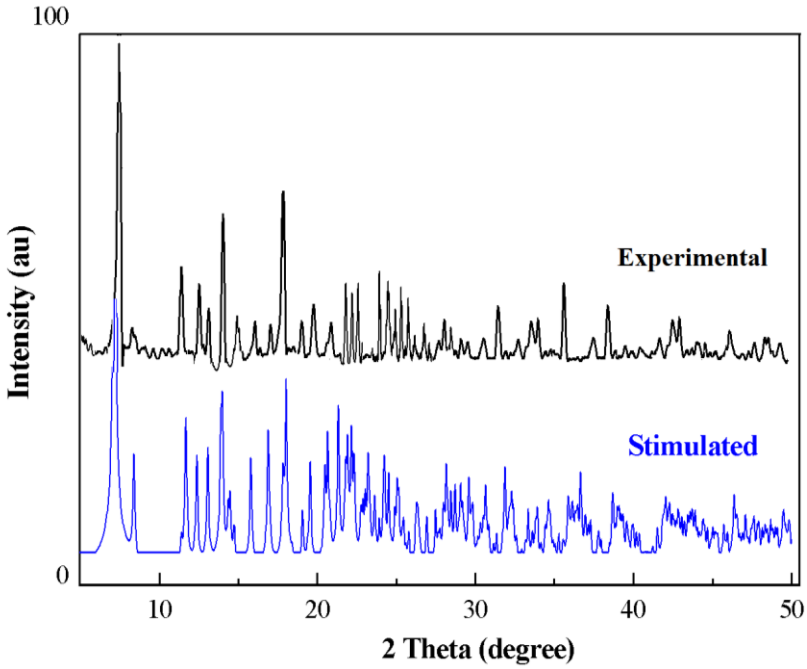

Figure S10. The X-ray powder diffraction diagrams of microcrystalline powders of **5**

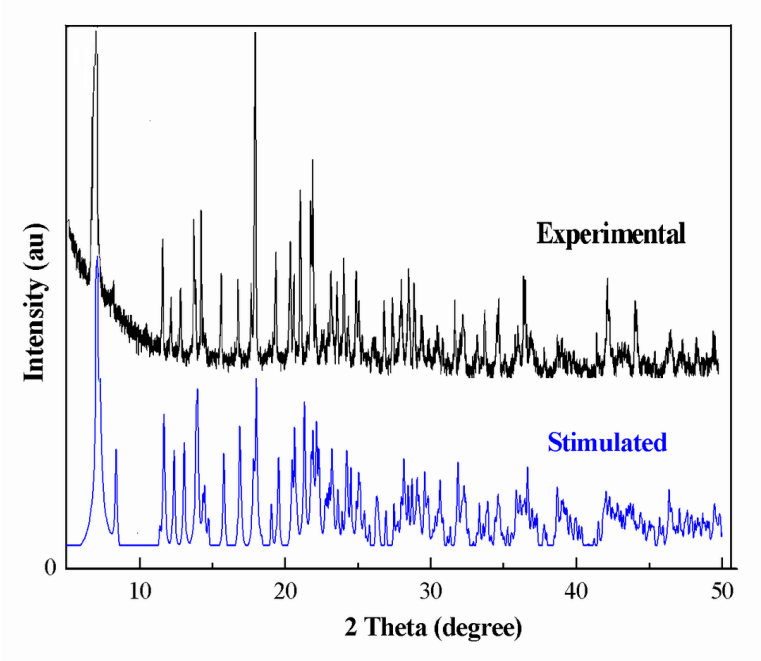

Figure S11. The X-ray powder diffraction diagrams of microcrystalline powders of **6**

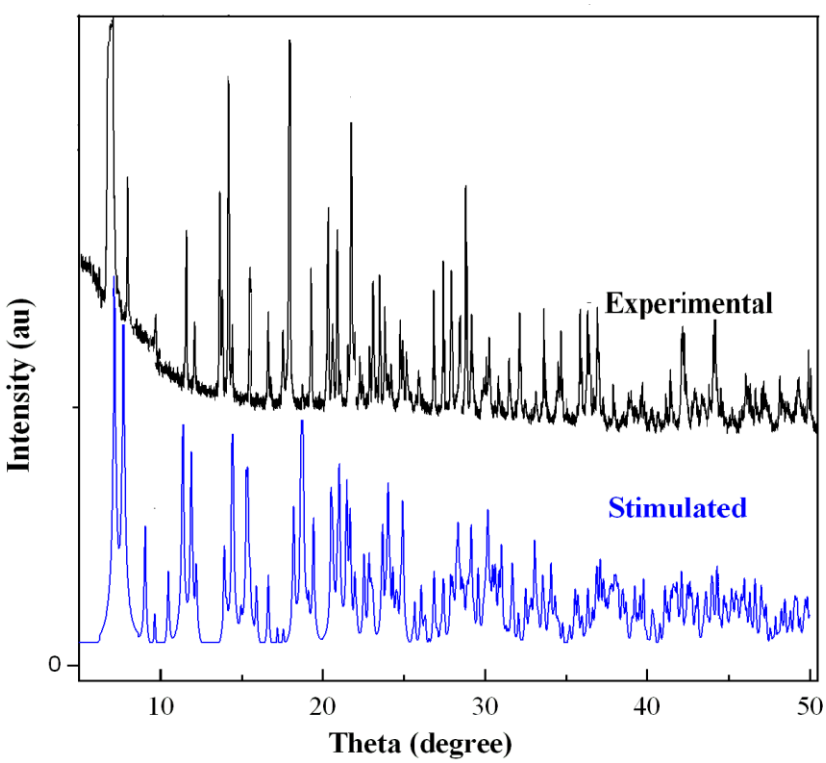

Figure S12. The X-ray powder diffraction diagrams of microcrystalline powders of **7**

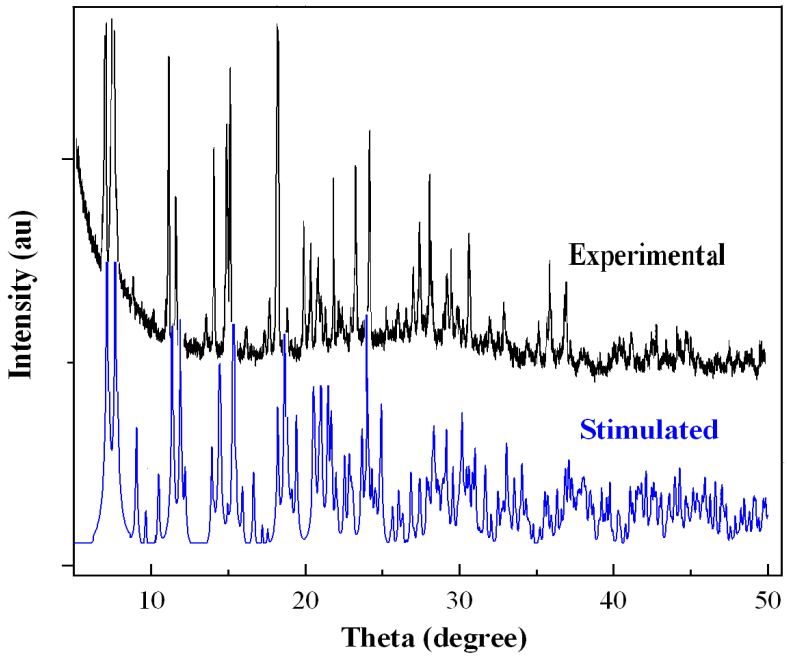

Figure S13. The X-ray powder diffraction diagrams of microcrystalline complexes **8**

The presence of water and thermal behavior of the complexes were further investigated by thermo analysis. The thermo-gravimetric/differential thermal analysis (TG-DTA) experiments were performed under N_2 atmosphere with a heating rate of 10 °C min^{-1} in the temperature range of 30–900 °C. As illustrated in Fig. S14, the TGA traces of complex **3** displays three major thermal events. The first mass loss of about 2.70 % in the region of 200 to 230 °C is attributed to the removal of the two coordinated water molecules (expected: 2.47 %). The second mass loss of ca. 35.0% in the region of 400–650 °C is maybe due to the decomposition of H_2PBDA ligands (expected: 34.3 %). An advanced degradation process takes place after 700 °C with the third mass loss of about 9.2%, presumably corresponding to the destruction of the two coordinated chloride anions. It is nearly in agreement with the calculated value of 9.1 %.

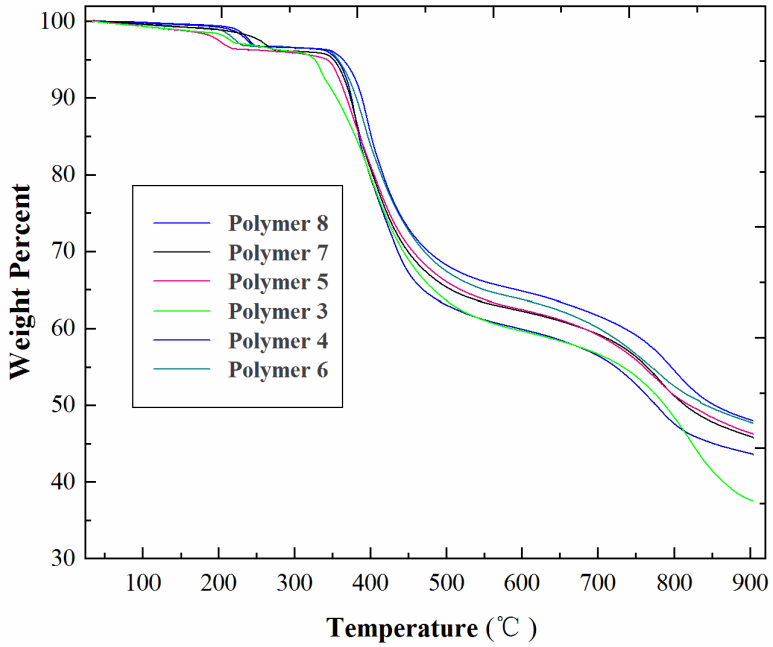

Figure S14. The thermogravimetric analyses (TGA) curves for complexes **3-8**

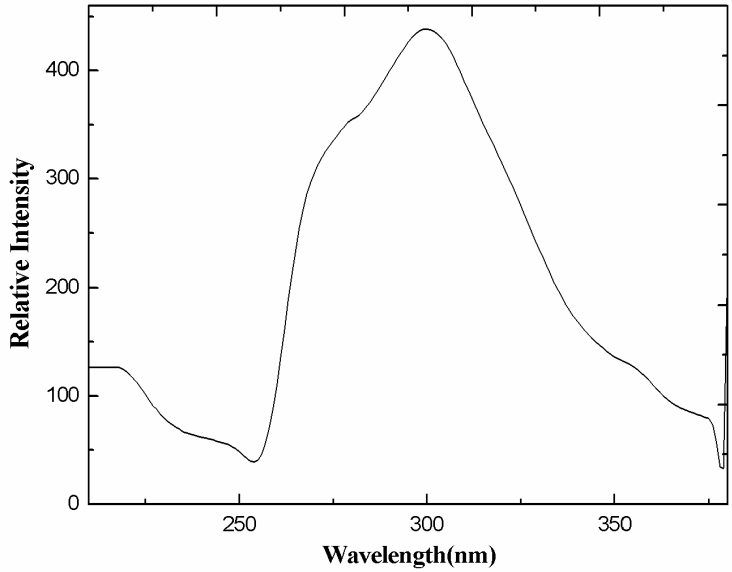

Figure S15. Photoemission spectra of the free PBDA ligand in DMF suspension state

Excitation of solid samples at 305 nm produces luminescence peaks with a maximum at 370 nm for **1** (see Figure. S16(b)). The fluorescence emission bands for **1** might be attributed to the intraligand emission from H_2PBDA, because the free H_2PBDA exhibits a luminescence at 308 nm

with the excitation at 279 nm. The enhancement of luminescence may be ascribed to ligand chelating to the metal centers, which effectively increases the rigidity of the ligand and reduces the loss of energy by radiationless decay.

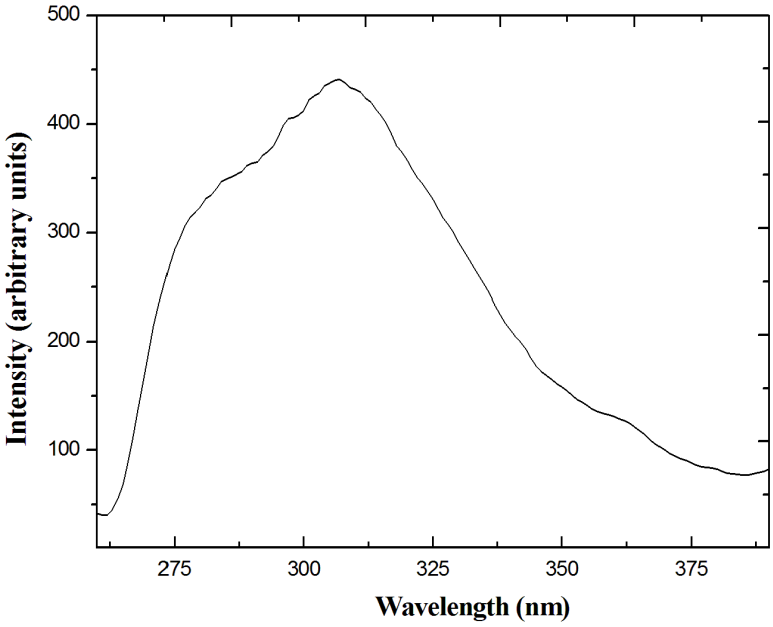

(a)

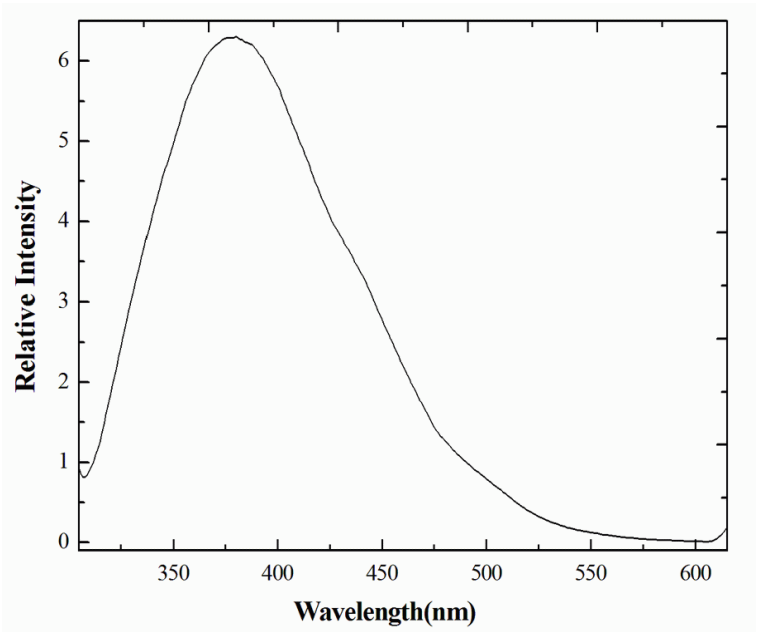

(b)

Figure S16. Photo excited (a) and emission (b) spectra of the complex Zn- HPBDA (**1**) in DMF suspension state

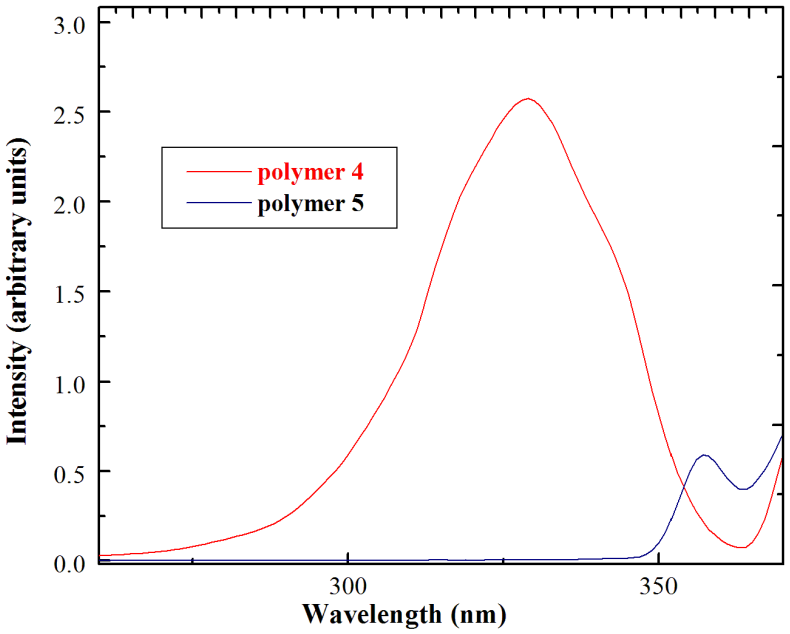

Figure S17. Photo excitation spectra of the complex **4** and **5** in DMF suspension

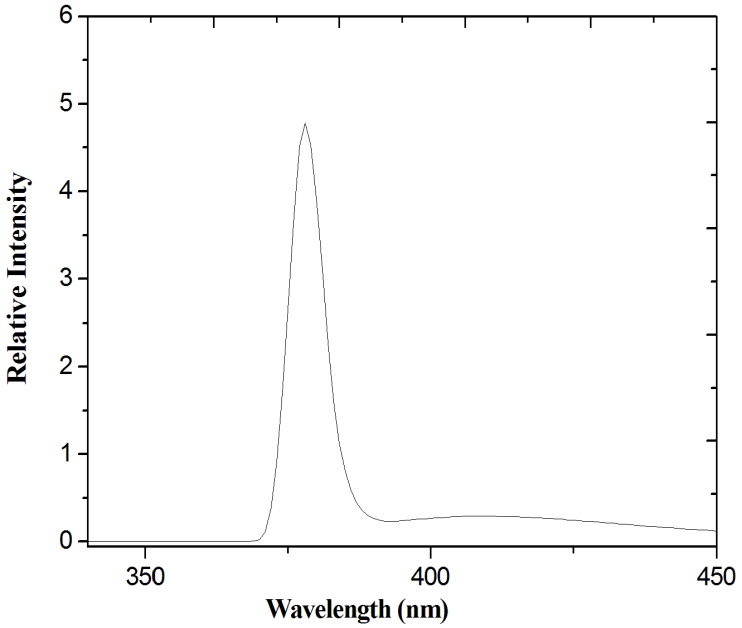

(a)

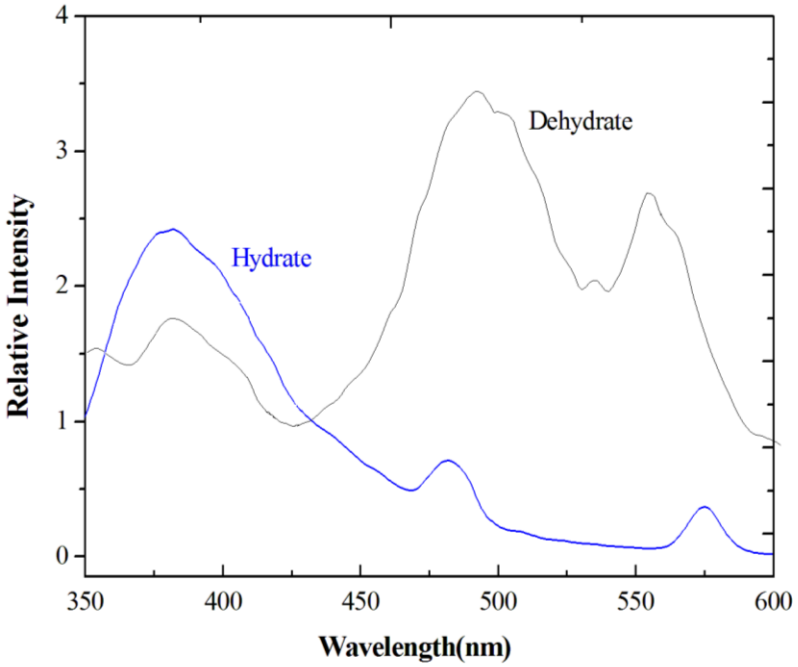

(b)

Figure S18. Photo excitation (a) and emission (b) spectra of complex **6** in DMF suspension state including the hydrate and dehydrate ones

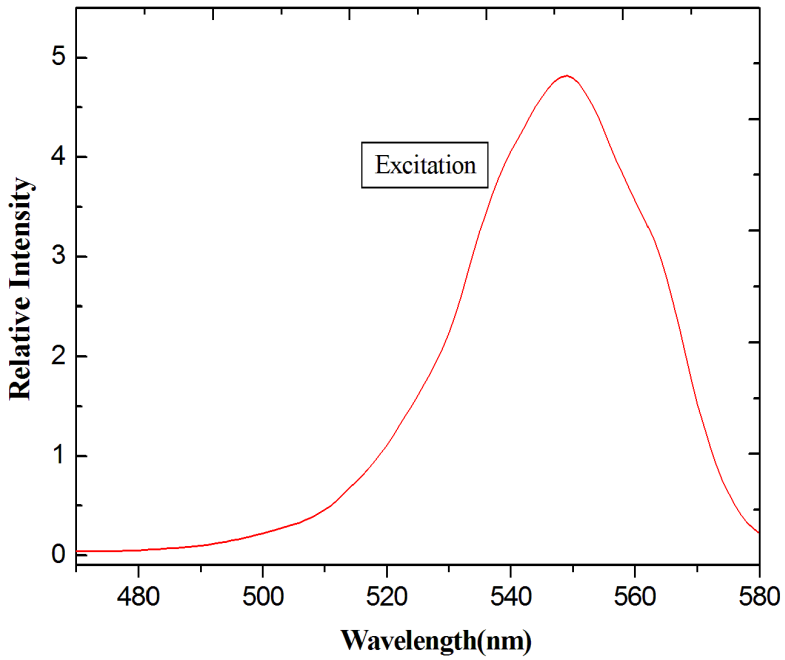

Figure S19. Photo excitation spectrum of complex **8** in DMF suspension

3 Supporting Magnetic Properties

For complex **3:**

There is no available expression to determine the magnetic susceptibilities of such 2D systems with large anisotropy. To obtain a rough quantitative estimation of the magnetic interaction between Nd(III) ions in **3**, the basic unit of **3** can also be considered as the mono- nuclear motif from the magnetic point of view, in which the Nd (III) ions are doubly linked through a pair of carboxylate bridges since the coupling through e are almost negligible due to the long distance. The Nd(III) ion may be assumed to exhibit a splitting of the m_j energy levels ($\hat{H} = \Delta \hat{J}_z^2$) in an axial crystal field.[2, 3] Thus, beyond 50 K the susceptibility data were fitted according to approximately the equation as following.

$$\chi_{Nd} = \frac{Ng^2\beta^2}{4kT} \times \frac{81e^{-81\Delta/4kT} + 49e^{-49\Delta/4kT} + 25e^{-25\Delta/4kT} + 9e^{-9\Delta/4kT} + e^{-\Delta/4kT}}{e^{-81\Delta/4kT} + e^{-49\Delta/4kT} + e^{-25\Delta/4kT} + e^{-9\Delta/4kT} + e^{-\Delta/4kT}} \quad ...(1)$$

eq **(**1)

$$x = J/kT \quad .... \quad .... \quad ..... \quad .... \quad .... \textbf{(}2)$$

In the expressions, Δ is zero-field splitting parameter, and the Zeeman splitting was treated isotropically for the sake of simplicity.

Equation (3) was assigned as a molecular field approximation

$$\chi = \frac{\chi'}{1-(2zj'/Ng^2\beta^2)\chi'} \quad . \quad ..... \quad .... \quad .... \textbf{(}3)$$

The least-squares analysis of the magnetic data gives Δ = –1.03 cm^{-1}, g = 0.77, zJ' = –0.31 cm^{-1} and $R = 3.65\times10^{-5}$.

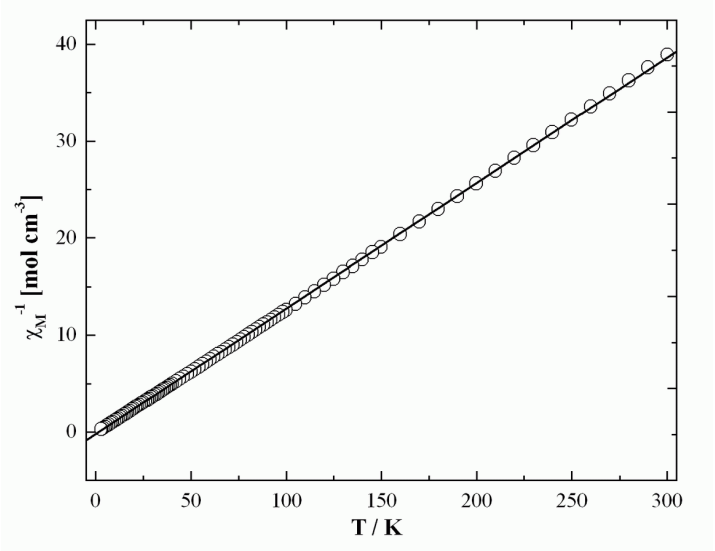

Figure S20. Temperature dependence of the inverse susceptibility between 2 and 300 K for complex **5**

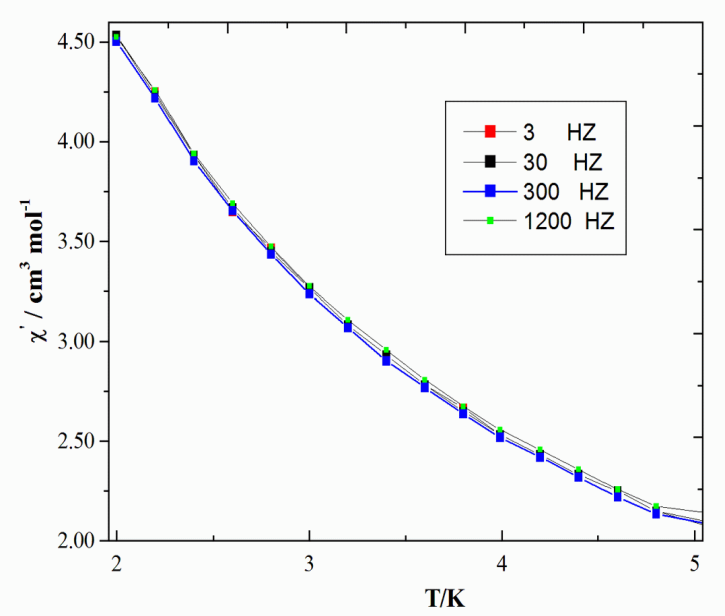

Figure S21: Temperature dependence of the in phase susceptibility for complex **6**

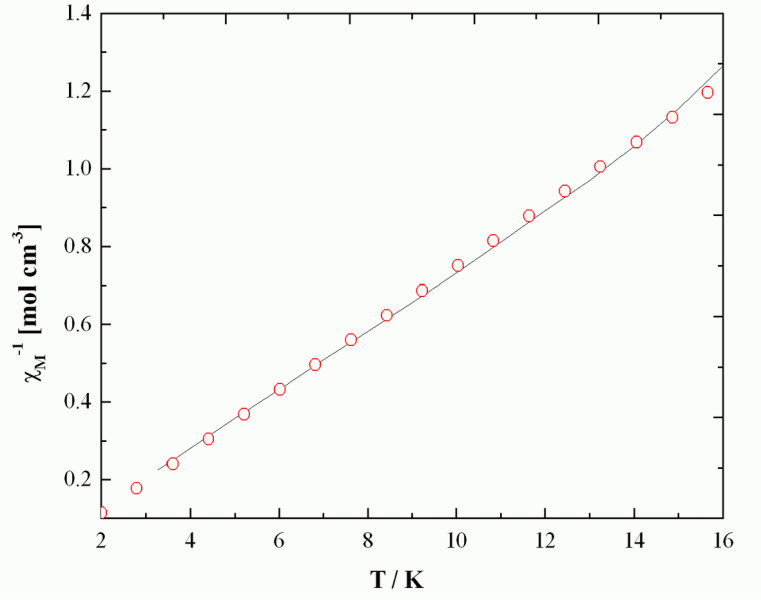

Figure S 22 Temperature dependence of the inverse susceptibility for complex **8** between 2 and 16 K

4 Additional Tables

Table S1 Selected bond lengths for complexes **1**–**8**

Complex **1**					
Zn(1)-O(6)	1.9304(19)	Zn(1)-O(3)#1	1.9387(19)	Zn(1)-O(1)	1.9515(18)
Zn(1)-N(1)#2	2.062(2)	O(3)-Zn(1)#3	1.9387(18)	N(1)-Zn(1)#4	2.062(2)
Complex **2**					
Pr(1)-O(4)	2.4389(16)	Pr(1)-O(3)	2.4641(17)	Pr(1)-O(11)	2.4761(17)
Pr(1)-O(8)	2.4852(16)	Pr(1)-O(9)	2.4943(16)	Pr(1)-O(5)#1	2.5456(17)
Pr(1)-O(10)#2	2.5673(17)	Pr(1)-O(9)#2	2.5788(16)	Pr(1)-O(4)#1	2.6489(15)
Zn(1)-O(7)	1.9801(17)	O(10)-Pr(1)#2	2.5673(17)	N(1)-Zn(1)#3	2.053(2)
Zn(1)-O(2)	1.9803(18)	Zn(1)-N(1)#3	2.053(2)	Zn(1)-Cl(1)	2.2209(8)
Complex **3**					
Nd(1)-O(3)	2.4207(15)	Nd(1)-O(2)	2.4527(17)	Nd(1)-O(11)	2.4632(17)
Nd(1)-O(7)	2.4675(16)	Nd(1)-O(8)	2.4851(15)	Nd(1)-O(4)#1	2.5305(17)
Nd(1)-O(9)#2	2.5543(17)	Nd(1)-O(8)#2	2.5597(15)	Nd(1)-O(3)#1	2.6357(15)
O(9)-Nd(1)#2	2.5543(17)	N(1)-Zn(1)#3	2.051(2)	Zn(1)-O(1)	1.9765(17)
Zn(1)-O(6)	1.9790(17)	Zn(1)-N(1)#3	2.051(2)	Zn(1)-Cl(1)	2.2204(7)
O(3)-Nd(1)#1	2.6357(15)	O(4)-Nd(1)#1	2.5305(17)	O(8)-Nd(1)#2	2.5597(15)
Complex **4**					
Eu(1)-O(2)	2.383(2)	Eu(1)-O(3)	2.407(2)	Eu(1)-O(8)	2.426(2)
Eu(1)-O(11)	2.428(2)	Eu(1)-O(7)	2.451(2)	Eu(1)-O(1)#1	2.486(2)
Eu(1)-O(6)#2	2.509(2)	Eu(1)-O(7)#2	2.518(2)	Eu(1)-O(2)#1	2.611(2)
Zn(1)-O(4)	1.972(2)	Zn(1)-O(9)	1.977(2)	Zn(1)-N(1)#3	2.041(3)
Zn(1)-Cl(1)	2.2189(10)	O(1)-Eu(1)#1	2.486(2)	O(2)-Eu(1)#1	2.611(2)
O(6)-Eu(1)#2	2.509(2)	O(7)-Eu(1)#2	2.518(2)	N(1)-Zn(1)#3	2.041(3)
Complex **5**					
Gd(1)-O(7)	2.3661(16)	Gd(1)-O(8)	2.4006(17)	Gd(1)-O(3)	2.4118(17)
Gd(1)-O(11)	2.4125(17)	Gd(1)-O(2)	2.4447(16)	Gd(1)-O(6)#1	2.4786(18)
Gd(1)-O(2)#2	2.5016(16)	Gd(1)-O(1)#2	2.5049(18)	Gd(1)-O(7)#1	2.6071(16)
O(7)-Gd(1)#1	2.6071(16)	N(2)-Zn(1)#3	2.048(2)	Zn(1)-O(9)	1.9742(18)
Zn(1)-O(4)	1.9766(18)	Zn(1)-N(2)#3	2.048(2)	Zn(1)-Cl(1)	2.2194(8)
O(1)-Gd(1)#2	2.5049(17)	O(2)-Gd(1)#2	2.5016(16)	O(6)-Gd(1)#1	2.4786(18)
Complex **6**					
Dy(1)-O(9)	2.435(4)	Dy(1)-O(8)	2.461(4)	Dy(1)-O(11)	2.476(4)
Dy(1)-O(2)#1	2.481(4)	Dy(1)-O(4)#1	2.495(4)	Dy(1)-O(10)#2	2.547(4)
Dy(1)-O(4)	2.568(4)	Dy(1)-O(5)	2.567(4)	Dy(1)-O(9)#2	2.644(4)
O(10)-Dy(1)#2	2.547(4)	N(2)-Zn(1)#3	2.048(5)	Zn(1)-O(7)	1.977(4)
Zn(1)-O(3)#1	1.983(4)	Zn(1)-N(2)#3	2.048(5)	Zn(1)-Cl(1)	2.2192(18)
O(2)-Dy(1)#1	2.481(4)	O(3)-Zn(1)#1	1.983(4)	O(4)-Dy(1)#1	2.495(4)
O(9)-Dy(1)#2	2.644(4)				

Complex **7**					
Ho(1)-O(10)#1	2.273(3)	Ho(1)-O(3)#2	2.293(3)	Ho(1)-O(11)	2.296(3)
Ho(1)-O(9)	2.316(3)	Ho(1)-O(8)	2.354(3)	Ho(1)-O(5)	2.382(3)
Ho(1)-O(4)#2	2.397(3)	Ho(1)-O(4)	2.603(3)	Zn(1)-O(2)#2	1.953(3)
Zn(1)-Cl(1)	2.1992(15)	Zn(1)-O(7)	1.976(3)	Zn(1)-N(1)#3	2.045(4)
Complex **8**					
Er(1)-O(9)#1	2.2650(18)	Er(1)-O(2)	2.285(2)	Er(1)-O(11)	2.290(2)
Er(1)-O(8)	2.3159(17)	Er(1)-O(7)	2.3490(17)	Er(1)-O(4)#2	2.372(2)
Er(1)-O(3)	2.3951(17)	Er(1)-O(3)#2	2.6026(17)	N(1)-Zn(1)#3	2.050(3)
Zn(1)-O(1)	1.957(2)	Zn(1)-O(6)	1.976(2)	Zn(1)-N(1)#3	2.050(3)
Zn(1)-Cl(1)	2.2073(10)	O(3)-Er(1)#2	2.6026(17)	O(4)-Er(1)#2	2.372(2)
O(9)-Er(1)#1	2.2650(18)				

Symmetry transformations used to generate equivalent atoms for **1**: #1 x,-y+1/2,z-1/2; #2 x,y,z-1; #3 x,-y+1/2,z+1/2; #4 x,y,z+1. for **2**: #1 -x,-y+1,-z; #2 -x+1,-y+1,-z; #3 -x+1,-y,-z. for **3**: #1 -x+2,-y,-z+1; #2 -x+1,-y,-z+1; #3 -x+1,-y+1,-z+1. for **4**: #1 -x,-y+1,-z+1; #2 -x+1,-y+1,-z+1; #3 -x+1,-y,-z+1. for **5**: #1 -x+2,-y+1,-z+1; #2 -x+1,-y+1,-z+1; #3 -x+1,-y+2,-z+1. for **6**: #1 -x+1,-y+1,-z+1; #2 -x,-y+1,-z+1; #3 -x+1,-y,-z+1. for **7**: #1 -x+1, -y,-z+1; #2 -x+2,-y,-z+1; #3 -x+1,-y+1,-z+1. for **8**: #1 -x+2,-y+2,-z; #2 -x+1,-y+2,-; z #3 x+1,y,z-1; #4 x-1, y, z+1.

Table S2 Selected bond Angles [°] for complexes **1**–**8**

Complex **1**					
O(6)-Zn(1)-O(3)#1	116.93(8)	O(6)-Zn(1)-O(1)	121.42(8)	O(3)#1-Zn(1)-O(1)	102.81(8)
O(6)-Zn(1)-N(1)#2	109.72(8)	O(3)#1-Zn(1)-N(1)#2	96.66(9)	O(1)-Zn(1)-N(1)#2	106.08(8)
Complex **2**					
O(4)-Pr(1)-O(3)	76.54(5)	O(4)-Pr(1)-O(11)	86.28(6)	O(3)-Pr(1)-O(11)	136.32(6)
O(4)-Pr(1)-O(8)	73.75(5)	O(3)-Pr(1)-O(8)	73.18(6)	O(11)-Pr(1)-O(8)	139.50(6)
O(3)-Pr(1)-O(9)	78.02(6)	O(11)-Pr(1)-O(9)	130.24(6)	O(8)-Pr(1)-O(9)	73.61(5)
O(4)-Pr(1)-O(5)#1	114.51(5)	O(11)-Pr(1)-O(5)#1	77.53(6)	O(8)-Pr(1)-O(5)#1	79.37(6)
O(9)-Pr(1)-O(5)#1	75.41(5)	O(4)-Pr(1)-O(10)#2	83.99(5)	O(3)-Pr(1)-O(10)#2	69.61(6)
O(11)-Pr(1)-O(10)#2	68.86(6)	O(9)-Pr(1)-O(10)#2	111.33(5)	O(5)#1-Pr(1)-O(10)#2	140.51(6)
O(3)-Pr(1)-O(9)#2	81.78(5)	O(11)-Pr(1)-O(9)#2	82.45(6)	O(8)-Pr(1)-O(9)#2	136.15(5)
O(9)-Pr(1)-O(9)#2	66.23(6)	O(4)-Pr(1)-O(4)#1	65.11(6)	O(3)-Pr(1)-O(4)#1	134.45(5)
O(11)-Pr(1)-O(4)#1	66.41(5)	O(8)-Pr(1)-O(4)#1	73.23(5)	O(9)-Pr(1)-O(4)#1	119.86(5)
O(7)-Zn(1)-O(2)	120.45(7)	O(7)-Zn(1)-N(1)#3	105.26(8)	O(2)-Zn(1)-N(1)#3	108.49(8)

O(7)-Zn(1)-Cl(1)	111.25(6)	O(2)-Zn(1)-Cl(1)	105.56(6)	N(1)#3-Zn(1)-Cl(1)	104.81(7)
Complex **3**					
O(3)-Nd(1)-O(2)	76.82(5)	O(3)-Nd(1)-O(11)	86.42(6)	O(2)-Nd(1)-O(11)	136.50(6)
O(3)-Nd(1)-O(7)	73.87(5)	O(2)-Nd(1)-O(7)	73.16(6)	O(11)-Nd(1)-O(7)	139.70(6)
O(2)-Nd(1)-O(8)	78.02(5)	O(7)-Nd(1)-O(8)	73.92(5)	O(11)-Nd(1)-O(8)	129.66(6)
O(11)-Nd(1)-O(4)#1	77.43(6)	O(3)-Nd(1)-O(4)#1	114.66(5)	O(2)-Nd(1)-O(4)#1	145.99(6)
O(7)-Nd(1)-O(4)#1	79.50(6)	O(8)-Nd(1)-O(4)#1	75.23(5)	O(3)-Nd(1)-O(9)#2	83.42(5)
O(2)-Nd(1)-O(9)#2	69.66(6)	O(11)-Nd(1)-O(9)#2	68.72(6)	O(7)-Nd(1)-O(9)#2	139.88(6)
O(8)-Nd(1)-O(9)#2	111.65(5)	O(3)-Nd(1)-O(8)#2	134.19(5)	O(2)-Nd(1)-O(8)#2	81.95(5)
O(11)-Nd(1)-O(8)#2	81.80(5)	O(7)-Nd(1)-O(8)#2	136.57(5)	O(8)-Nd(1)-O(8)#2	66.34(6)
O(8)-Nd(1)-O(3)#1	120.03(5)	N(1)#3-Zn(1)-Cl(1)	104.90(7)	O(3)-Nd(1)-O(3)#1	64.98(6)
O(2)-Nd(1)-O(3)#1	134.53(5)	O(11)-Nd(1)-O(3)#1	66.53(5)	O(7)-Nd(1)-O(3)#1	73.27(5)
O(1)-Zn(1)-O(6)	120.25(7)	O(1)-Zn(1)-N(1)#3	107.91(8)	O(6)-Zn(1)-N(1)#3	105.78(8)
O(1)-Zn(1)-Cl(1)	105.82(6)	O(6)-Zn(1)-Cl(1)	111.16(6)		
Complex **4**					
O(2)-Eu(1)-O(3)	77.61(7)	O(2)-Eu(1)-O(8)	74.59(7)	O(3)-Eu(1)-O(8)	73.20(7)
O(2)-Eu(1)-O(11)	86.15(7)	O(3)-Eu(1)-O(11)	137.21(8)	O(8)-Eu(1)-O(11)	139.59(7)
O(3)-Eu(1)-O(7)	77.80(7)	O(8)-Eu(1)-O(7)	74.56(7)	O(11)-Eu(1)-O(7)	128.68(8)
O(2)-Eu(1)-O(1)#1	114.87(7)	O(8)-Eu(1)-O(1)#1	79.37(7)	O(11)-Eu(1)-O(1)#1	77.14(8)
O(7)-Eu(1)-O(1)#1	75.03(7)	O(2)-Eu(1)-O(6)#2	82.28(7)	O(3)-Eu(1)-O(6)#2	69.80(8)
O(11)-Eu(1)-O(6)#2	68.93(8)	O(7)-Eu(1)-O(6)#2	111.84(7)	O(2)-Eu(1)-O(7)#2	134.20(7)
O(3)-Eu(1)-O(7)#2	82.48(7)	O(8)-Eu(1)-O(7)#2	136.95(7)	O(11)-Eu(1)-O(7)#2	81.19(7)
O(7)-Eu(1)-O(7)#2	65.78(8)	O(2)-Eu(1)-O(2)#1	64.49(8)	O(3)-Eu(1)-O(2)#1	134.44(7)
O(8)-Eu(1)-O(2)#1	73.09(7)	O(11)-Eu(1)-O(2)#1	66.55(7)	O(7)-Eu(1)-O(2)#1	120.60(7)
O(2)-Eu(1)-C(20)#2	107.56(8)	O(3)-Eu(1)-C(20)#2	73.72(8)	O(11)-Eu(1)-C(20)#2	74.03(8)
O(7)-Eu(1)-C(20)#2	88.99(8)	O(4)-Zn(1)-O(9)	119.78(9)	O(4)-Zn(1)-N(1)#3	107.22(11)
O(9)-Zn(1)-N(1)#3	106.84(11)	O(4)-Zn(1)-Cl(1)	106.19(7)	O(9)-Zn(1)-Cl(1)	111.07(8)
Complex **5**					
O(7)-Gd(1)-O(8)	77.84(6)	O(7)-Gd(1)-O(3)	74.57(6)	O(8)-Gd(1)-O(3)	73.26(6)
O(7)-Gd(1)-O(11)	86.36(6)	O(8)-Gd(1)-O(11)	137.47(6)	O(8)-Gd(1)-O(2)	77.77(6)
O(3)-Gd(1)-O(2)	74.87(5)	O(11)-Gd(1)-O(2)	128.16(6)	O(7)-Gd(1)-O(6)#1	114.78(6)
O(3)-Gd(1)-O(6)#1	79.44(6)	O(11)-Gd(1)-O(6)#1	76.81(6)	O(2)-Gd(1)-O(6)#1	75.11(6)
O(7)-Gd(1)-O(2)#2	134.22(6)	O(8)-Gd(1)-O(2)#2	82.49(6)	O(3)-Gd(1)-O(2)#2	137.12(5)
O(11)-Gd(1)-O(2)#2	80.95(6)	O(2)-Gd(1)-O(2)#2	65.62(6)	O(7)-Gd(1)-O(1)#2	82.18(6)
O(8)-Gd(1)-O(1)#2	69.80(6)	O(11)-Gd(1)-O(1)#2	69.07(6)	O(2)-Gd(1)-O(1)#2	111.78(5)
O(7)-Gd(1)-O(7)#1	64.27(6)	O(8)-Gd(1)-O(7)#1	134.48(6)	O(3)-Gd(1)-O(7)#1	73.09(5)
O(11)-Gd(1)-O(7)#1	66.52(6)	O(2)-Gd(1)-O(7)#1	120.86(5)	O(9)-Zn(1)-O(4)	119.48(7)
O(9)-Zn(1)-N(2)#3	106.69(9)	O(4)-Zn(1)-N(2)#3	107.51(9)	O(9)-Zn(1)-Cl(1)	106.28(6)

O(4)-Zn(1)-Cl(1)	111.22(6)	N(2)#3-Zn(1)-Cl(1)	104.62(7)		
Complex **6**					
O(9)-Dy(1)-O(8)	76.47(13)	O(9)-Dy(1)-O(11)	86.10(14)	O(8)-Dy(1)-O(11)	136.09(15)
O(9)-Dy(1)-O(2)#1	73.86(13)	O(8)-Dy(1)-O(2)#1	73.27(14)	O(8)-Dy(1)-O(4)#1	78.10(14)
O(11)-Dy(1)-O(4)#1	130.31(15)	O(9)-Dy(1)-O(10)#2	114.51(13)	O(11)-Dy(1)-O(10)#2	77.64(15)
O(9)-Dy(1)-O(4)	134.27(13)	O(8)-Dy(1)-O(4)	81.80(13)	O(11)-Dy(1)-O(4)	82.42(13)
O(2)#1-Dy(1)-O(4)	136.21(13)	O(4)#1-Dy(1)-O(4)	66.18(15)	O(10)#2-Dy(1)-O(4)	105.94(13)
O(9)-Dy(1)-O(5)	83.84(13)	O(8)-Dy(1)-O(5)	69.61(14)	O(11)-Dy(1)-O(5)	68.66(15)
O(4)#1-Dy(1)-O(5)	111.31(13)	O(4)-Dy(1)-O(5)	50.76(13)	O(9)-Dy(1)-O(9)#2	65.14(15)
O(8)-Dy(1)-O(9)#2	134.38(13)	O(11)-Dy(1)-O(9)#2	66.51(13)	O(5)-Dy(1)-O(9)#2	126.20(13)
O(7)-Zn(1)-O(3)#1	120.51(18)	O(7)-Zn(1)-N(2)#3	108.4(2)	O(7)-Zn(1)-Cl(1)	105.56(14)
O(3)#1-Zn(1)-Cl(1)	111.30(14)	N(2)#3-Zn(1)-Cl(1)	104.75(16)		
Complex **7**					
O(9)#1-Er(1)-O(2)	81.55(8)	O(9)#1-Er(1)-O(11)	70.92(7)	O(2)-Er(1)-O(11)	110.82(9)
O(9)#1-Er(1)-O(8)	77.26(6)	O(2)-Er(1)-O(8)	81.82(7)	O(2)-Er(1)-O(7)	82.54(7)
O(8)-Er(1)-O(7)	72.85(6)	O(11)-Er(1)-O(4)#2	87.70(9)	O(8)-Er(1)-O(4)#2	79.13(7)
O(7)-Er(1)-O(4)#2	87.03(7)	O(9)#1-Er(1)-O(3)	129.13(6)	O(2)-Er(1)-O(3)	75.75(6)
O(11)-Er(1)-O(3)	75.68(7)	O(7)-Er(1)-O(3)	72.75(6)	O(4)#2-Er(1)-O(3)	116.95(6)
O(2)-Er(1)-O(3)#2	138.64(6)	O(11)-Er(1)-O(3)#2	72.23(7)	O(8)-Er(1)-O(3)#2	121.55(6)
O(7)-Er(1)-O(3)#2	74.35(6)	O(3)-Er(1)-O(3)#2	64.92(7)	O(11)-Er(1)-C(8)#2	80.79(9)
O(8)-Er(1)-C(8)#2	99.42(7)	O(7)-Er(1)-C(8)#2	77.95(7)	O(3)-Er(1)-C(8)#2	91.13(7)
O(1)-Zn(1)-O(6)	122.09(9)	O(1)-Zn(1)-N(1)#3	111.72(11)	O(6)-Zn(1)-N(1)#3	95.68(10)
O(1)-Zn(1)-Cl(1)	105.83(8)	O(6)-Zn(1)-Cl(1)	110.78(7)	N(1)#3-Zn(1)-Cl(1)	110.34(8)
Complex **8**					
O(10)#1-Ho(1)-O(11)	70.84(10)	O(3)#2-Ho(1)-O(11)	111.10(13)	O(10)#1-Ho(1)-O(9)	77.44(10)
O(3)#2-Ho(1)-O(9)	81.87(11)	O(3)#2-Ho(1)-O(8)	82.28(11)	O(9)-Ho(1)-O(8)	72.63(9)
O(10)#1-Ho(1)-O(5)	99.46(11)	O(11)-Ho(1)-O(5)	87.72(12)	O(9)-Ho(1)-O(5)	78.92(10)
O(8)-Ho(1)-O(5)	86.88(10)	O(11)-Ho(1)-O(4)#2	75.92(11)	O(8)-Ho(1)-O(4)#2	72.85(9)
O(5)-Ho(1)-O(4)#2	117.05(9)	O(10)#1-Ho(1)-O(4)	133.81(10)	O(3)#2-Ho(1)-O(4)	138.56(10)

Table S3 The hydrogen bond lengths (Å) and angles (°) for complexes **2-8**

D-H...A	d(D-H)	d(H...A)	d(D...A)	<(DHA)
Complex **2**				
O(11)-H(2W)...O(8)#1	0.85	2.05	2.850(2)	157.3
O(11)-H(1W)...N(2)#4	0.85	1.95	2.767(3)	160.5
Complex **3**				
O(11)-H(1W)...N(2)#4	0.85	1.93	2.765(3)	168.2
O(11)-H(2W)...O(7)#1	0.85	2.03	2.848(2)	160.4
Complex **4**				
O(11)-H(1W)...O(8)#1	0.85	2.04	2.843(3)	157.2
O(11)-H(2W)...N(2)#4	0.85	1.98	2.776(4)	156.1
Complex **5**				
O(11)-H(1W)...O(3)#1	0.86	2.00	2.846(2)	167.4
O(11)-H(2W)...N(1)#4	0.88	1.93	2.783(3)	164.2
Complex **6**				
O(11)-H(1W)...O(2)#4	0.85	2.02	2.841(6)	161.4
O(11)-H(2W)...N(1)#5	0.85	1.95	2.755(7)	157.1
Complex **7**				
O(11)-H(1W)...N(2)#4	0.82	1.97	2.739(3)	157.0
O(11)-H(2W)...O(7)#2	0.96	1.78	2.680(3)	155.6
Complex **8**				
O(11)-H(2W)...O(8)#2	0.85	1.88	2.683(4)	156.1
O(11)-H(1W)...N(2)#5	0.85	1.91	2.732(5)	161.6

Symmetry codes for **2**: #1 -x,-y+1,-z; #4 x, y, z-1. for **3**: #1 -x+2,-y,-z+1; #4 x, y, z+1. for **4**: #1 -x,-y+1,-z+1; #4 x, y, z-1. for **5**: #1 -x+2,-y+1,-z+1; #4 x,y,z+1. for **6**: #4 x-1,y,z; #5 -x+1,-y+1,-z. for **7**: #2 -x+2,-y,-z+1; #4 x,y,z+1. for **8**: #2 -x+1,-y+2 ,-z; #5 x, y+1, z.

Table S4 The parameters for aromatic stacking interactions for complexes **1-8**

Parameters	Listing atoms included in the adjacent aromatic rings	The centre to centre distance (Å)	Dihedral angle between the adjacent planes (°)	Centre-to-plane distance (Å)
Complex **1**	$C_9C_{10}C_{11}C_{12}C_{13}N_1$ and $C_2C_3C_4C_5C_6C_7$	3.647	10.94	3.856
Complex **2**	$C_{22}C_{23}C_{24}C_{25}C_{26}N_{20}$ and $C_{22}C_{23}C_{24}C_{25}C_{26}N_2$	3.611	0	3.603
Complex **3**	$C_9C_{10}C_{11}C_{12}C_{13}N_1$ and $C_9C_{10}C_{11}C_{12}C_{13}N_1$	3.889	0	3.790
Complex **4**	$C_9C_{10}C_{11}C_{12}C_{13}N_1$ and $C_9C_{10}C_{11}C_{12}C_{13}N_1$	3.806	0	3.805
Complex **5**	$C_{22}C_{23}C_{24}C_{25}C_{26}N_2$ and $C_{22}C_{23}C_{24}C_{25}C_{26}N_2$	3.903	0	3.812
Complex **6**	$C_{22}C_{23}C_{24}C_{25}C_{26}N_2$ and $C_{22}C_{23}C_{24}C_{25}C_{26}N_2$	3.901	0	3.784
Complex **7**	$C_9C_{10}C_{11}C_{12}C_{13}N_1$ and $C_9C_{10}C_{11}C_{12}C_{13}N_1$	4.071	0	4.678
Complex **8**	$C_9C_{10}C_{11}C_{12}C_{13}N_1$ and $C_9C_{10}C_{11}C_{12}C_{13}N_1$	4.679	0	4.103

References

(1) Li, H. R. Fronczek, F. R. Vicente, M. G. H. C J. Organomet. Chem., **2009**, 694, 1607.

(2) O'Connor, C. J. *Prog. Inorg. Chem*. **1982**, *29*, 203.

(3) Casey, A. P. in: Boudreaux, E. A. Mulay, L.N. (Eds.), Theory and Applications of Molecular Paramagnetism, John Wiley, New York, **1976**, p. 27.